Available online at www.sciencedirect.com

ScienceDirect

MATTER AND RADIATION AT EXTREMES

Matter and Radiation at Extremes 2 (2017) 139–148

www.journals.elsevier.com/matter-and-radiation-at-extremes

Research Article

Experimental investigation of the reaction-build-up for plastic bonded explosive JOB-9003

Xu Zhang [a,*,1], Yanfei Wang [b], Feng Zhao [a], Rong Zhang [a], Bin Zhong [a]

[a] *National Laboratory of Shock Wave and Detonation Physics, Institute of Fluid Physics, China Academy of Engineering Physics, Mianyang, Sichuan, 621900, China*

[b] *Graduate School of China Academy of Engineering Physics, Mianyang, Sichuan, 621900, China*

Received 17 February 2016; revised 5 September 2016; accepted 14 September 2016
Available online 6 March 2017

Abstract

In order to measure the shock initiation behavior of JOB-9003 explosives, Al-based embedded multiple electromagnetic particle velocity gauge technique has been developed. In addition, a gauge element called the shock tracker has been used to monitor the progress of the shock front as a function of time, thus providing a position–time trajectory of the wave front as it moves through the explosive sample. The data is used to determine the position and time for shock to detonation transition. All the experimental results show that the rising-up time of Al-based electromagnetic particle velocity gauge is very short (<20 ns); the reaction-build-up velocity profiles and the position–time for shock to detonation transition of HMX-based plastic bonded explosive (PBX) JOB-9003 with 1–8 mm depth from the origin of the impact plane under different initiation pressures were obtained with high accuracy.

PACS codes: TJ55; O38

Keywords: Embedded electromagnetic particle velocity gauge; JOB-9003 explosive; Particle velocity profile

1. Introduction

Accurate numerical modeling of high explosive detonation is an important goal to replace the high empirical models with physically accurate numerical calculations. A useful model of detonation process should have enough accuracy, stability and insensitivity to details of modeling such as artificial viscosity, the mesh aspect ratio or the mesh spacing. Considering reacting flow with a wide range of time and length scales is necessary. Moreover, a standard reactive flow model describing a detonating explosive as a continuous medium should obey the conservation of mass, momentum, and energy, together with the equation of state (EOS) for reactant, reactive explosive, and global heat-release reaction rate equation. To infer the specific information on the global heat-release rate for shock to detonation transition, experiments that can record the reaction-build-up processes of explosives are necessary to obtain an empirical form for the global heat-release rate. Therefore, lots of reaction-build-up processes experiments [1–5] of explosives have been investigated based on several techniques. Generally, the most widely used techniques are manganin pressure gauges, embedded electromagnetic particle velocity gauge and laser interferometric technique. These techniques can be used to record pressures or particle velocities, which help calibrate the build-up to detonation reaction rate parameters of explosives.

* Corresponding author.
E-mail address: caepzx@sohu.com (X. Zhang).

Peer review under responsibility of Science and Technology Information Center, China Academy of Engineering Physics.

[1] Research Field: reactive fluid dynamics, shock wave and detonation physics, ultrafast experimental techniques.

http://dx.doi.org/10.1016/j.mre.2017.02.001

2. Background

Plate impact experiments are widely used over the past several decades to gain an understanding of shock to detonation transition under shock loading. Generally, the flat plate impact experiments are performed with a power-driven gun or a light gas gun to provide a well characterized one-dimensional impact pressure in the explosive sample, which can shock-load materials to GPa for tens of μs over sample volumes of cm^3 depending on the propulsion method adopted. They are also precision devices providing well-defined loading impulse over times relevant to all the operating mechanisms which enable kinetics to be deduced from the response to the loading. The input pulse in experimental samples can be square with a duration determined by twice of the flyer thickness divided by the appropriate wave speed of the flyer. In addition, powder-driven guns and gas guns are capable of loading samples whose size and duration are limited by the dimension of the device.

In order to track the reaction-build-up as a function of time and depth of energetic materials, in-situ gauging techniques and laser interferometric techniques have been developed and carried out at different national laboratories in the past. In-situ gauging techniques, *i.e.* magnetic particle velocity gauges [6−18], manganin pressure gauges [19], PVDF [20−23] and quartz [24−27], can measure at several Lagrangian positions in a single experiment. Using these techniques, pressure or particle velocity measurements can be made at several Lagrangian positions during shock to detonation transition. The waveforms represent valuable information related to the homogeneous/heterogeneous nature of the reaction-build-up process. These studies give information about the reaction rates based on one-dimensional Lagrange analysis and refinements in the global reaction rate models, and are valuable to provide data calibrating the reactive models which simulate the initiation of explosives.

In-situ manganin pressure gauges, as the most common device directly recording stress histories at a point in the reactive flow of energetic materials, have been used for many years. The most commonly used pressure gauge at >10 GPa pressure in shock to detonation of energetic materials is manganin alloy gauge, which is made of alloy of copper, zinc and manganese, with high dependence of resistance on pressure [25] and negligible dependence on temperature. The manganin gauges can measure the full stress tensor behind shock wave front because they can be mounted at different orientations [27] to the motion of the shock front. To sense the longitudinal stress pulse passing the gauge location, generally H-, π-shaped and grid (see Fig. 1(b)) gauges are used. The grid gauge etched on a glass fiber with a 5-μm-thick manganin foil is embedded between target tiles. A perpendicular plane shock wave can sweep across the active region of the grid gauge, which has an active element of 1 mm width with 48 Ω resistance. In addition, a manganin piezoresistive foil pressure gauge placed within the explosive sample normally needs to be armored with sheets of Teflon insulation on each side of the gauge to protect the manganin piezoresistive foil. To sense the lateral stress, generally

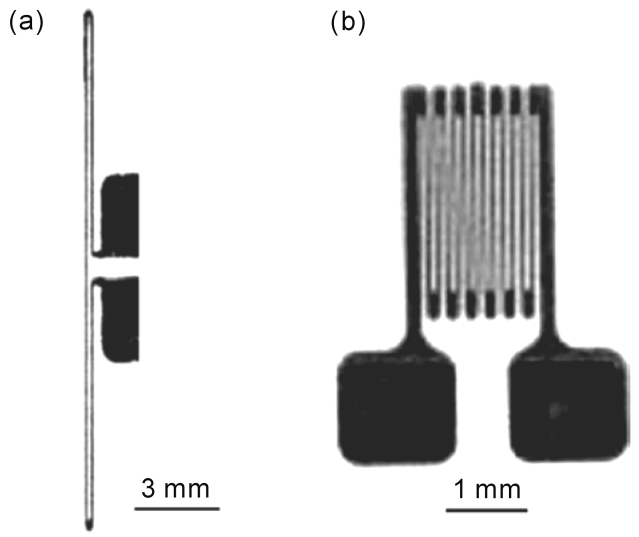

Fig. 1. (a) T-shaped manganin pressure gauge and (b) grids manganin pressure gauges.

T-shaped gauges (see Fig. 1(a)) with 100-μm-thick insulating sheets mounted in a cut perpendicular to the shock plane are used. The entire gauge can be equilibrated with the stress field in ~200 ns before the gauge reaches equilibration. Therefore, the major disadvantage of the manganin gauges is that rapidly evolving features of the shock or detonation wave front could be missed because of internal mounting of the gauges in the sample, where the time response of the gauge layer in the sample may take ~200 ns. In addition, polyvinylidene difluoride (PVDF) and quartz which is based on piezoelectric response have also been used to measure shock stresses, which have similar disadvantages as the manganin gauges.

Using the measured shock velocity and particle velocity history data to construct Hugoniot or to calibrate reaction rate model parameters is another important method being extensively used. The laser interferometric technique and in-situ magnetic particle velocity gauging are two commonly used methods to measure the history of particle velocity in shock wave and detonation physics. In the laser interferometric technique, focused laser incident on the target material is used to collect and couple shifted light into the fiber, and the velocity history is furthermore deduced based on the observed free surface velocities.

Commonly used optical diagnostics include the velocity interferometer system for any reflector (VISAR) and photonic Doppler velocimetery (PDV). In the VISAR, the Doppler shifted light is divided into two beams with different optical paths and recombines at the photodetector, incorporating a large-core, multi-mode fiber, leading to a high light collection efficiency. In addition, the characteristics of the large core fiber are insensitive to variations on the polarization of input light. The main advantage of VISAR is its ability to measure any velocity produced by land-based projectiles. In contrast to VISAR, PDV is advantageous due to its short rise-time, typically on the order of 100 ps depending on the detector, electronic cabling and digitizer, and other components (as shown in Fig. 2). PDV lacks the ability to measure very high velocity.

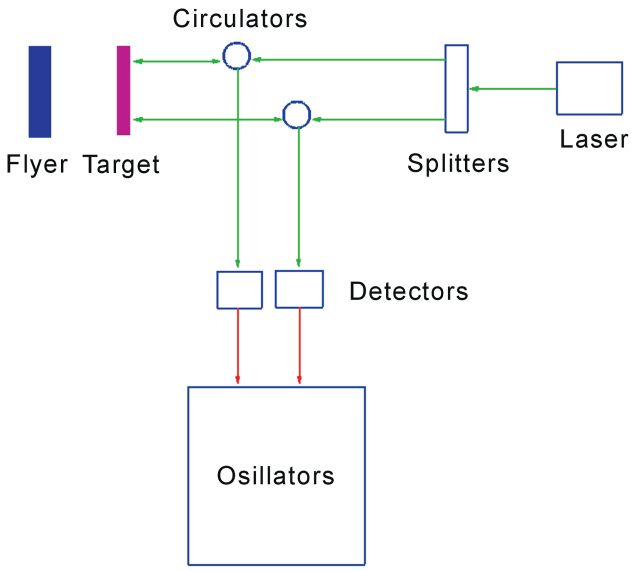

Fig. 2. Photonic Doppler velocimeter principle.

Short response time (on the order of 2 ns) which is non-invasive is the main advantage of both PDV and VISAR. However, these two techniques can only make measurements in the direction of shock or detonation propagation, and impossible to make internal measurements.

In-situ electromagnetic particle velocity gauge technique is an important tool to study shock detonation transition and aging effects of explosive. As an imbedding type sensor, its main characteristics are high sensitivity and no need for calibration. The first practical demonstration of this technique was in the early 1960s by Zaitzev et al. [1], who used a gauge made from a conducting loop to measure the particle velocity during explosively generated shocks. Before the technique was taken up by Vorthman and his colleagues [2,3], the particle velocity gauges were not used widely. A series of experiments in comparison with other measurement techniques done by Erickson et al. [4] showed that particle velocity gauge was a viable method. The importance of the leads orientation to the magnetic field, which could be affected by specimen assembly methods, was demonstrated in their experiments. Moreover, Gupta et al. [5] developed the techniques to measure the particle velocity profiles due to compression and shear waves through pressure-shear loading. Fowles and Williams [6] was the first to use this technique on gas gun, then Vorthman [2], Campbell [7], Dick [8] and Gustavsen [9,10] at LANL applied this method to study the shock detonation transition of different kind of explosives, and recorded particle velocity profiles under different initiation pressures. Subsequently, particle velocity gauges have been used to study large numbers of energetic materials, mostly by Sheffield, Gustavsen, Alcon and their co-workers [28–32] and others from LANL [33]. At the same time, temperature effects, granular size effects and aging effects were considered in their work, and Hugoniot curve of reactant explosive and POP relationship are also given in these experimental results.

In the Institute of Fluid Physics (IFP) in China, previous electromagnetic particle velocity gauges were made of Cu [34–38], and the loading method was based on the explosive driven flyer which resulted in large noise and slow time response. In the following sections of this paper, the development of the capability measuring particle velocities via Al-based electromagnetic gauges up to 8 Lagrangian positions in a single experiment will be described. The reactive wave growth for the plastic bonded explosive (PBX) JOB-9003 has been recorded from the initial impact shock through the build-up process, to nearly a full detonation. In addition to the particle velocity, the wave front position as a function of time as obtained in a traditional explosive wedge experiment is recorded with shock tracker gauges. In the next few years, these gauges will be used for the measurement of the shock and detonation transition properties of insensitive energetic materials.

3. Electromagnetic particle velocity gauge technique

3.1. Experimental principle and method

The particle velocity gauges work based on a simple physical principle, as a voltage will be induced in the circuit as part of the loop cuts magnetic field lines when it moves, when a conductor in a closed loop moves in a magnetic field. The output voltage depends on the magnetic field strength, the length of the conductor which cuts the field lines, and the velocity of movement. The relation can be written as

$$v = 10^3 \varepsilon / Bl \tag{1}$$

where v (mm/μs) is the particle velocity; ε (V) is the induced voltage; l (mm) is the length of active element; B (T) is the magnetic field strength. ε as a function of time, is recorded during the experiment. B and l are measured before the experiment, then the active element velocity v as a function of time can be determined. Assuming that the active element moves with the reactive flow of explosive that it is embedded in, the particle velocity of the explosive sample at that particular Lagrangian position can be determined.

The experimental device of the particle velocity gauges includes the gas-gun and vacuum targets room, Lexon sabots, sapphire flyer (Φ = 55 mm), protection cylinder, wedged explosive sample (Φ = 40 mm × 30 mm), particle velocity gauges, and 0.14 T permanent magnetic device (as shown in Fig. 3(a) and (b)). The explosive sample is machined with a bottom and top shape so that the gauge membrane can be glued at an angle of 30° with respect to the shock plane. In order to measure the input wave, a single gauge is mounted on the impact plane of the sample, parallel to the shock plane. A target plate on which the explosive sample is mounted is placed in the gun target chamber. It is located between the pole pieces of a large permanent magnet. The permanent magnetic device has a non-homogeneous degree of <1% over a 30 mm length in a cubic region. The explosive sample is positioned specifically to make the gauge ends perpendicular to the field lines (as shown in Fig. 3(a)), so that the gauge leads won't cut the field lines as they move, otherwise the leads movement will affect the measured voltage signal and cause errors.

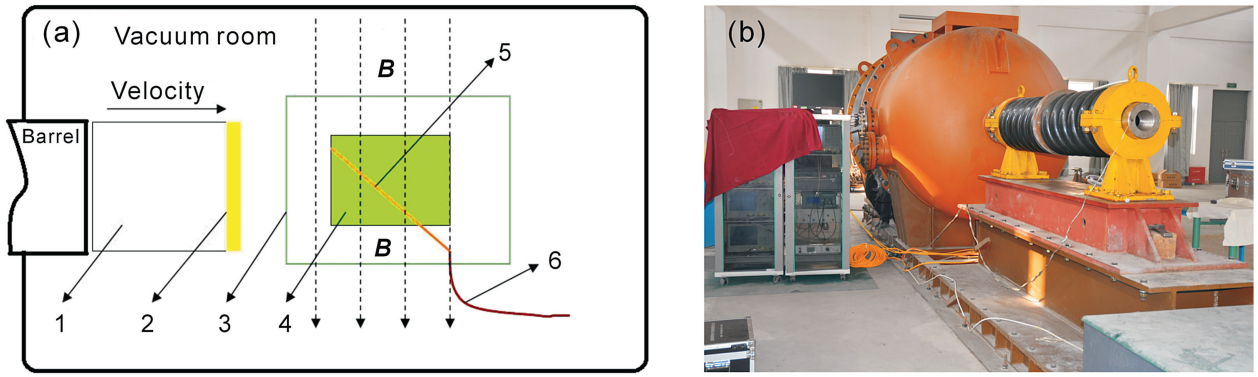

Fig. 3. (a) Scheme of the experimental device of the particle velocity gauges. 1 – Lexon sabots. 2 – flyer. 3 – protection cylinder. 4 – HMX-based explosive sample. 5 – electromagnetic particle velocity gauge. 6 – conducting wire. (b) Photo of the experimental device.

3.2. Al-based electromagnetic particle velocity gauge

A typical multiple electromagnetic particle velocity gauge configuration is shown in Fig. 4, which includes 8 particle velocity gauges (25 μm thick), orientated orthogonally to the magnetic field, with the leads perpendicular to the gauge elements to prevent experiencing an imposed voltage during shock loading. The gauge elements of particle velocity gauges nest one inside the other. They are spaced at 2 mm intervals. The horizontal part of each gauge produces a net voltage which is called an active element. The length of the active elements ranges from 5 to 12 mm, therefore the active elements are spaced 1 mm apart and cover depths of ~1–8 mm with the origin at the impact surface, and are mounted at 30° between the explosive wedges (see Fig. 5(a) and (b)).

In addition, the electromagnetic particle velocity gauge also contains three shock tracer gauges. One is located on either side of the nested particle velocity gauges and the other was located in the center of the gauges. The length of the active element changes with the wave propagates through the shock tracker gauge. The output voltage will be high when the conductor is relatively long, and low when the conductor is short, because of the change of the corresponding voltage related to the shock position. Thus a time–distance diagram of the shock wave propagates through the sample can be recorded.

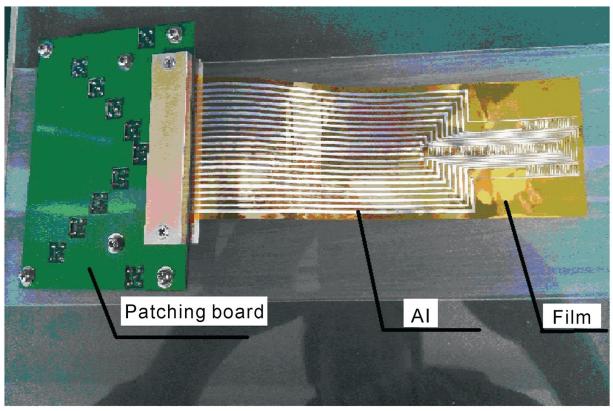

Fig. 4. Al-based electromagnetic particle velocity gauge.

Moreover, a single gauge with a single particle velocity element is mounted on a plane parallel to the impact surface to measure the particle velocity at the impacting surface. The single gauge providing a measurement of the input shock characteristics has an active element of 10 mm long.

3.3. Impact pressure calculation

Impact pressures of all the experiments were calculated with the impedance matching technique, which was based on the fact of the same pressure p and particle velocity u_p between the impactor and target. The initiation pressures in the impactor and explosive sample target were calculated based on

$$\begin{aligned} P_1 &= \rho_{01} D_1 \left(u_{imp} - u_p\right), \\ P_2 &= \rho_{02} D_2 \, u_p \, , \end{aligned} \tag{2}$$

where subscripts 1 and 2 represent the impactor and target respectively, D is the shock velocity, u_p is the particle velocity on the impact interface, u_{imp} is the velocity of the impact, and ρ_0 is the initial density. For the impactor and target, the calculation of the relationship of the shock velocity achieved for a particular input driving velocity uses the linear D-u_p equation of state

$$D = a + b\, u_p, \tag{3}$$

where a and b are constants specific for a certain material. Constants for sapphire used as the material of the impactor and JOB-9003 explosive are listed in Table 1. Interface pressure and particle velocity can be solved based on the measured velocity of impactor by solving

$$\begin{aligned} P_1 &= \rho_{01} \left[a_1 + b_1 \left(u_{imp} - u_p\right)\right] \left(u_{imp} - u_p\right), \\ P_2 &= \rho_{02} \left(a_2 + b_2 \, u_p\right) u_p \, , \end{aligned} \tag{4}$$

The thickness of the sapphire impactor is 12 mm, which guarantees that the rarefaction fan originates at the back of impact cannot reach the shock front since the shock to detonation transition occurs. A representation of a one-dimensional sapphire impactor and targets is shown as a distance-time (x–t) diagram in Fig. 6. In addition, the project

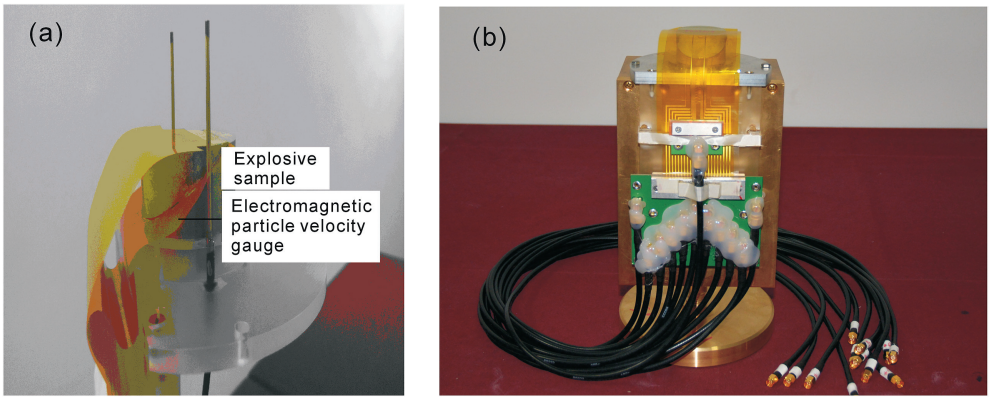

Fig. 5. Electromagnetic particle velocity gauge in the explosive sample.

impact velocity (u_{imp}) was measured with the optical technique.

4. Results and discussions

4.1. Time response of Al-based electromagnetic particle velocity gauge

Generally, time response of Al-based electromagnetic particle velocity gauge is determined by the time of the active element accelerated to the velocity of surrounding media, the angle between the shock wave and active element, and the response time of the electronic cable and recording system. Time response of the active element is determined by twice the shock wave reflection time in the active element, $t_1 = 4\delta/D$, where D is the shock wave velocity, δ is the thickness of the active element. Movement of the active element from initial to full-speed is determined by the angle between the shock wave and active element, as $t_2 = l\cdot\sin\theta/D$, where l is the length of active element, θ is the angle between the shock wave and active element. For example, the shock wave velocity in the sample is $D = 5.25$ mm/μs, the angle between the shock wave and active element is 0.5°, the thickness of the active element is $\delta = 10$ μm, and the response time of the active element is $t_1 \approx 7.62$ ns and $t_2 \approx 18$ ns, then the total response time is ~0–30 ns. In this study, four different initiation pressures 3.07, 4.14, 7.81, 8.12 GPa in the explosive sample were tested, with no tilt angle between the shock wave and active element. As shown in Fig. 7, for 4.14 GPa initiation pressure and 1 mm depth in the explosive sample, the active element, left shock trace gauge and right shock tracer gauge almost have the same time response, which means that there is no tilt angle between the shock wave and active element. The total response time of the active element is ~20 ns (shown in Fig. 8).

Table 1
Hugoniot parameters for sapphire used as the material of impactor and JOB-9003 explosive.

Material	ρ_0	a	b
Sapphire	3.985	11.19	1
JOB-9003	1.845	2.17	1.99

In addition, to study the effect of different materials of the active element, an experiment using a 10-μm-thick Al active element was compared with the same experiment but with Cu active element. In the experiments, the active elements of Al and Cu were installed on the impact surface, which guaranteed the flyer arriving at the active elements at the same time. The result is shown in Fig. 9 with the impact pressure of 8.71 GPa. As can be seen in Fig. 9, the time response of Al active element is 0.06 μs, while that of Cu active element is 0.07 μs, which means that the response of Al active element is 7% faster than the Cu one. Therefore, using Al as the material for the active element of electromagnetic particle velocity gauge is better than Cu.

4.2. Hugoniot data of PMMA measured with Al-based electromagnetic particle velocity gauge

Hugoniot Data of PMMA were measured to estimate the response property and accuracy of Al-based electromagnetic particle velocity gauge. As an example, the particle velocity profiles of PMMA with the impact velocity of 580 m/s are

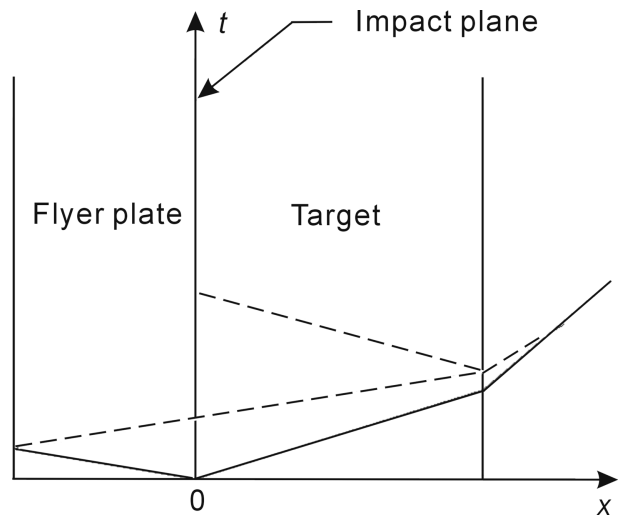

Fig. 6. Lagrangian representation of shock experiments: x–t diagram. The impact is at $t = 0$ and shock wave travels into the flyer plate to the left ($x < 0$) and target to the right ($x > 0$). Reflection leads to a release fan.

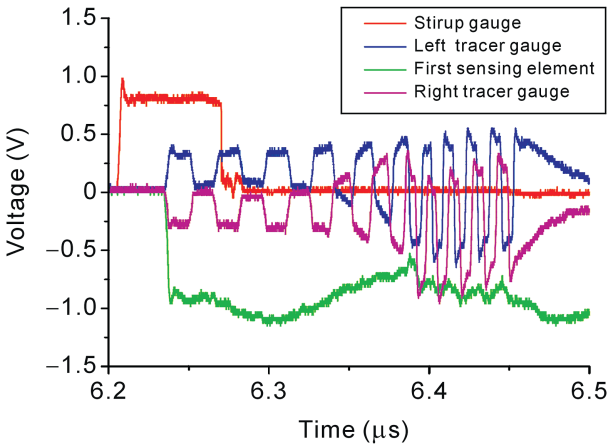

Fig. 7. Time responses of the active element, left and right shock trace gauge and Al-based electromagnetic particle velocity gauge.

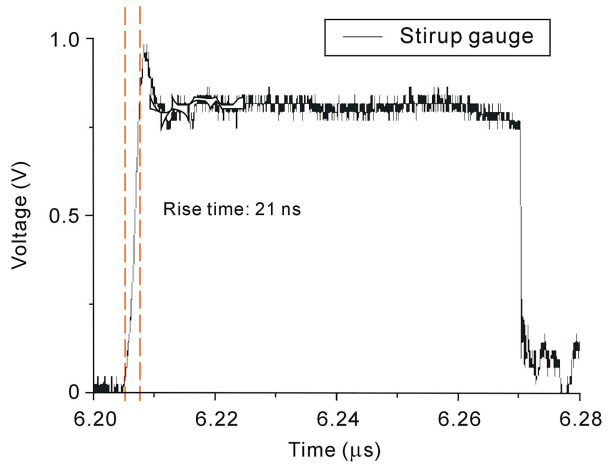

Fig. 8. Time response of Al-based electromagnetic particle velocity gauge.

presented in Fig. 10, where each trace has been corrected for its active length using Equation (1). In this figure, the traces are regularly spaced, showing that the shock velocity in PMMA is constant and flat topped, with no rounding as the particle velocity reaches its maximum.

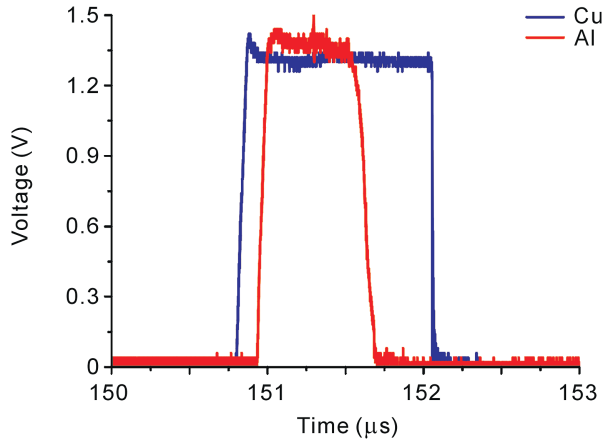

Fig. 9. Time responses of Cu and Al as the active element material of electromagnetic particle velocity gauges.

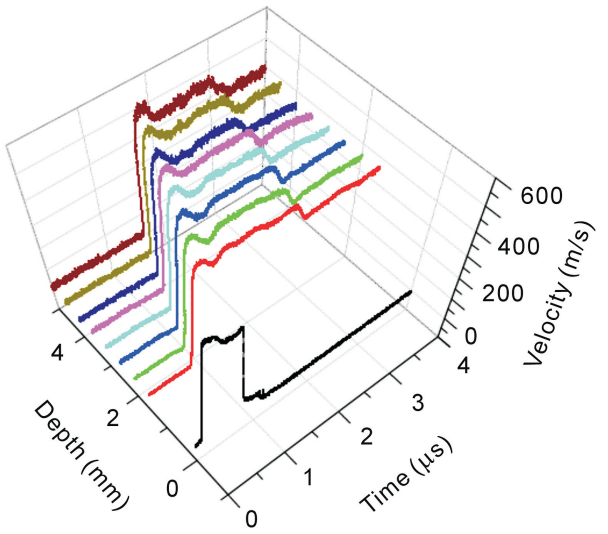

Fig. 10. Particle velocity profiles of PMMA with the impact velocity of 580 m/s.

The shock velocity (measured by the gradients of the distance–time plots in Fig. 10) and the particle velocity (calculated from the height of the gauge traces in Fig. 10) of PMMA are shown in Fig. 11. The measured date was compared with accepted Hugoniot data for PMMA published by Barker and Hollenbach [40–42], who used an interferometric system to measure the rear surface velocity of the specimen. The two data sets agree to a reasonable degree, although there is a small degree of scattering in both cases.

Overall, the results from the Al-based electromagnetic particle velocity gauge and shock tracker gauges show that these gauges have produced accurate results in PMMA, and can be used in energetic materials with enough confidence.

4.3. Particle velocity profiles of HMX-based explosive under different initiation pressures

All the JOB-9003 shots were done on a 57-mm bore powered gun. This allowed experiments of 40 mm diameter to be conducted. The particle velocity gauge is used to provide accurate particle velocity–time traces at different locations within a target during shock to detonation transition. A number of experiments have been completed for JOB-9003 at several different input shock levels from ~3.07 to 8.12 GPa. Fig. 12 gives good original records of shock to detonation transition for PBX-based explosive JOB-9003, which shows

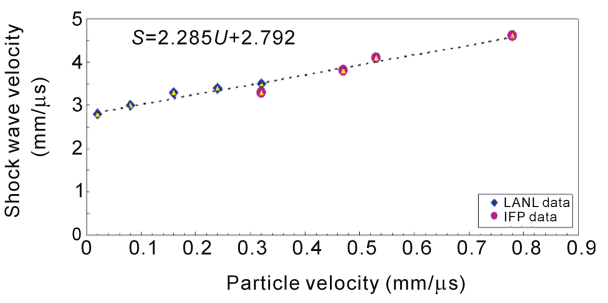

Fig. 11. Hugoniot data of PMMA.

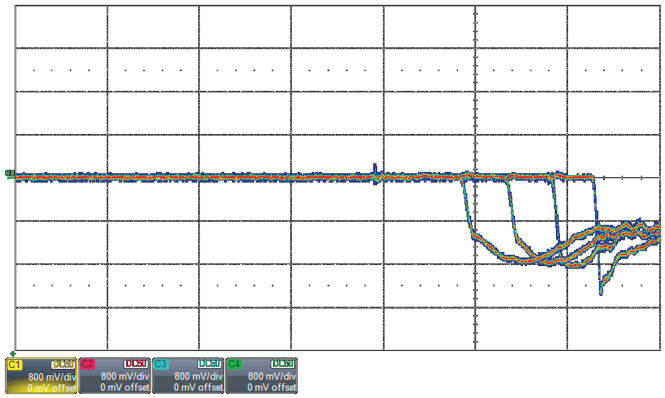

Fig. 12. Records of shock to detonation transition for PBX-based explosive.

Table 2
Sample density and impact pressure conditions.

Sample density (g/cm^3)	Shock wave velocity (km/s)	Interface velocity (m/s)	Impact pressure (GPa)
1.849	3.165	525	3.07
1.841	3.460	650	4.14
1.845	3.846	1101	7.81
1.845	3.876	1136	8.12

the waveforms from an experiment in which JOB-9003 was impacted by a sapphire impactor at a velocity of 0.576 mm/μs producing an input to the explosive of 3.07 GPa. There are 4 waveforms from the gauges that were at the depths of 1–4 mm into the explosive from the multiple embedded gauges. The waveforms clearly indicate that significant reactions occurred during the gauge measurements.

Four shots of HMX-based explosive JOB-9003 under different initiation pressures are listed in Table 2, where the initiation pressures range from 3.07 to 8.12 GPa. The initial sample densities are also listed in Table 2.

The single gauge was placed on the impact plane and therefore showed the initial particle velocity. The multiple electromagnetic particle velocity gauges were placed in the sample from 1 mm to 8 mm depth. The original voltage signals of HMX-based explosives under initiation pressures of 3.07, 4.14, 7.81 and 8.12 GPa are shown in Fig. 13(a)–(d) respectively. It can be seen that the original voltage signals have high accuracy and low noise. The corresponding particle velocity profiles are shown in Fig. 14(a)–(d). All the curves show a time response of <20 ns, which means that the designed multiple electromagnetic particle velocity gauges are suitable for recording the Lagrange velocity profiles of shock to detonation. The first trace of each curve in Fig. 14 shows the particle velocity profile on the impact plane. All the active elements of multiple electromagnetic particle velocity gauges are spaced 1 mm apart and covered a depth of 8 mm from the origin of the impact plane. As seen in Fig. 14(a), at low initiation pressure of 3.07 GPa, the particle velocity profile does not show an increase in the depth of 1 mm, and later the reaction is evident as the rounded hump is behind the initial shock. However, the reaction hump doesn't catch up with the inert shock wave. As shown in Fig. 14(b), the JOB-9003 input is 4.14 GPa and it causes the explosive sample to initiate fast enough and nearly reaches a detonation by the time when the

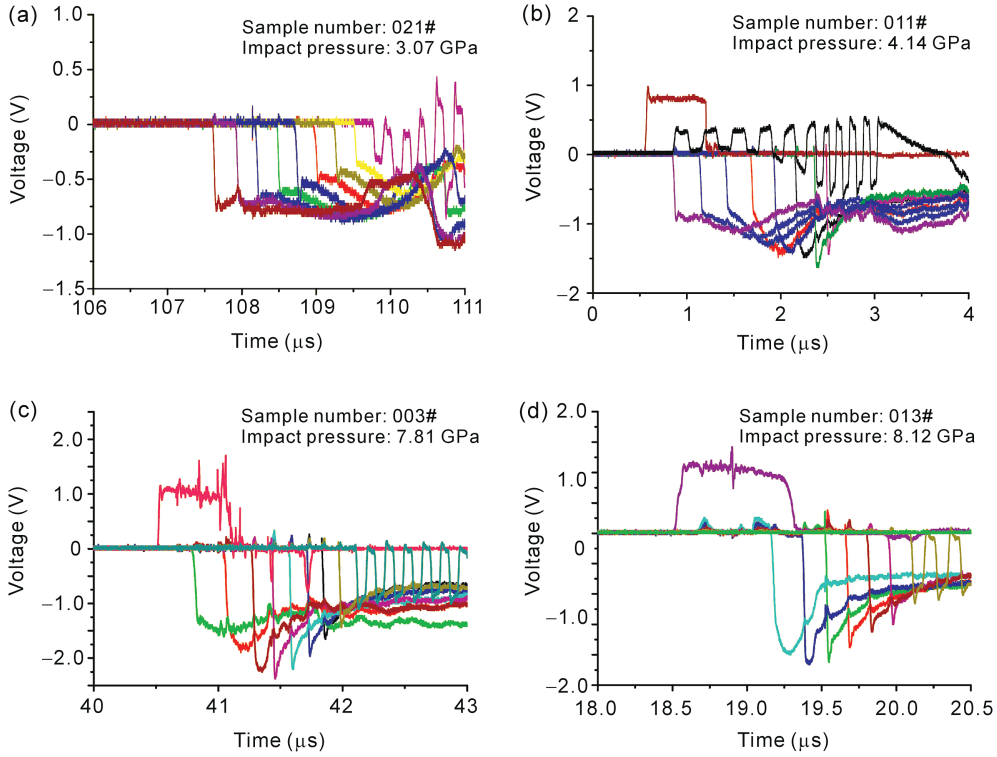

Fig. 13. Al-based electromagnetic particle velocity gauge signals in explosive build-up for input pressures of (a) 3.07 GPa, (b) 4.14 GPa, (c) 7.81 GPa and (d) 8.12 GPa.

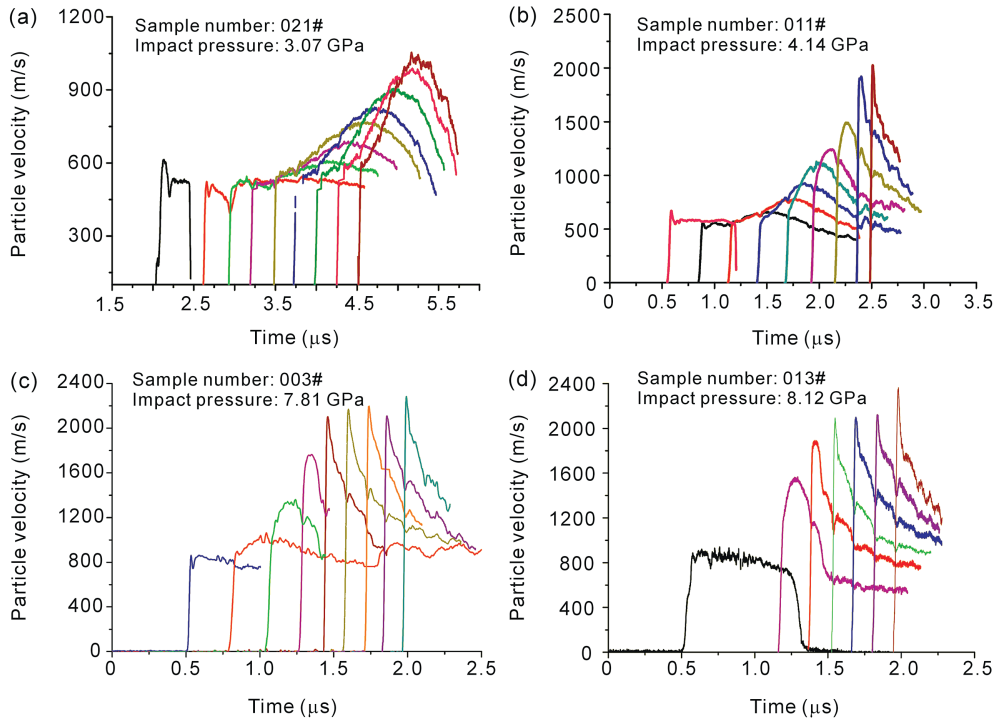

Fig. 14. Particle velocities of impact pressures at (a) 3.07 GPa, (b) 4.14 GPa, (c) 7.81 GPa, (d) 8.12 GPa.

wave traverses the last gauge at a position of ~8 mm into the explosive. Moreover, for the initiation pressures of 4.14, 7.81 and 8.12 GPa, the hump grows in the particle velocity and finally catches up with the initial inert precursor shock wave. The magnitude of the shock at the shock front also grew as it travels deeper into the explosive sample. Onset of detonation happens when the reaction hump catches up the initial inert precursor shock wave. Particle velocity profiles on the detonation are right angles with a peak particle velocity >2.0 km/s.

4.4. JOB-9003 shock tracker data

Another important aim of this experimental is to study the design and implementation of a shock tracker. The signal from the shock tracker gauge consists of an oscillating voltage signal with time, the periodicity of which gives a direct measure of the shock velocity as the spacing of each measuring element in the shock tracker is precisely known. This is demonstrated in Fig. 15(a). Therefore, simply by measuring the time at a constant voltage, it is possible to determine the shock velocity. The original data of the shock tracer gauges for the initiation impact pressure of 4.14 GPa is shown in Fig. 15(a). As the shock front passes over each element, the output goes from high to low (or low to high). In addition, a rather large perturbation on the data can be seen due to the transition to detonation process. This perturbation does not significantly hinder the interpretation of the position–time information. The position of the shock wave front with time shown in Fig. 15(b) is derived from Fig. 15(a). The data about the wave arrival time of particle velocity gauge provides position–time measurements in every 1.0 mm change and the shock tracker gauge information provide position–time measurements in every 0.5 mm change. Lines have been drawn through the data indicating the unreacted shock velocity (initial slope) and the detonation velocity (final slope). Onset of

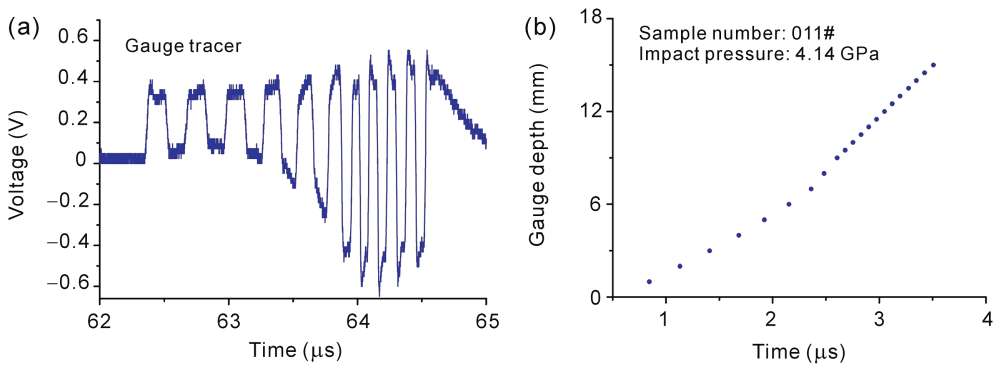

Fig. 15. (a) Gauge tracer signal and (b) propagation of shock wave in the sample.

detonation is indicated by a change of slope, where the initial shallow slope is the initial inert precursor shock wave, and the subsequent deep slope is the detonation velocity. The inflection point represents the onset of detonation. Since a detonation proceeds after the transition, a measurement of the detonation velocity is also possible. Moreover, the early part of the shock tracker data can be used to provide the shock velocity for the unreacted explosive. With the input particle velocity and this measurement, an unreacted Hugoniot point can be determined.

Clearly, the experimental data shows that the multiple magnetic gauge technique can provide a rich harvest of data from each shot, and these data include unreacted states, the reactive wave evolution, the reactive wave front acceleration, and the transition to a detonation. The information will be helpful to model the behavior of shock to detonation transition process.

6. Conclusions

Al-based multiple electromagnetic particle velocity gauges are developed. They have much shorter response time and a higher accuracy than Cu-based multiple electromagnetic particle velocity gauges. Based on the Al-based multiple electromagnetic particle velocity gauges, particle velocity profiles of an HMX-based PBX explosive under four different initiation pressures are recorded, which show the shock to detonation transition procedure. The experimental results can be used to calibrate reaction rate parameters and validate the numerical simulation code of shock to detonation transition.

Acknowledgments

We thank Professor Yihong Hang, Professor Heng Yu, and Professor Xin Yu worked at Institute of Applied Physics and Computation Mathematics for their support in this project. The development of the experiments was funded by China Academy of Engineering Physics.

References

[1] V.M. Zaitzev, P.F. Pokhil, K.K. Shvedov, The Electromagnetic Method for the Measurements of Velocities of Detonation Products, DAN SSSR 132 1339, 1960.

[2] J.E. Vorthman, Facilities for the study of shock induced decomposition of high explosives, in: L. Seaman, R.A. Graham (Eds.), Shock Waves in Condensed Matter, American Institute of Physics, New York, 1981, p. 680.

[3] J. Vorthman, G. Andrews, J. Wackerle, Reaction rates from electromagnetic gauge data, in: J.M. Short (Ed.), Proc. 8th Symp. (Int.) on Detonation, Naval Surface Weapons Center, Silver Spring, MD, 1980, pp. 99−110.

[4] L.M. Erickson, W.L. Parker, H.C. Vantine, K.C. Weingart, R.S. Lee, The electromagnetic velocity gauge: use of multiple gauges, time response, and flow perturbations, in: J.M. Short (Ed.), Proc. 7th Symp. (Int.) on Detonation, Naval Surface Weapons Center, Dahlgren, VA, 1981, pp. 1062−1071.

[5] Y.M. Gupta, D.D. Keough, D.F. Walter, K.C. Dao, D. Henley, A. Urweider, Experimental facility to produce and measure compression and shear waves in impacted solids, Rev. Sci. Instrum. 51 (1980) 183−194.

[6] R. Fowles, R.F. Williams, Plane wave stress propagation in solids, J. Appl. Phys. 41 (1) (1970) 360−365.

[7] A.W. Campbell, W.C. Davis, J.B. Ramsay, F.R. Travis, Shock initiation of solid explosive, Phys. Fluids 21 (4) (1961) 511−577.

[8] J.J. Dick, C.A. Forest, J.B. Ramsay, W.L. Seitz, The Hugoniot and shock sensitivity of a plastic-bonded TATB explosive PBX 9502, J. Appl. Phys. 63 (1988) 4881−4887.

[9] R.L. Gustavsen, S.A. Sheffield, R.R. Alcon, Measurements of shock initiation in the tri-amino-tri-nitro-benzene based explosive PBX 9502: wave forms from embedded gauges and comparison of four different material lots, J. Appl. Phys. 99 (2006) 114907.

[10] R.L. Gustavsen, S.A. Sheffield, R.R. Alcon, Low pressure shock initiation of porous HMX for two grain size distributions and two densities, in: American Institute of Physics (AIP) Conference Proceedings, 1995.

[11] S.A. Sheffield, R.R. Alcon, R.L. Gustavsen, R.A. Graham, M.U. Anderson, Particle velocity and stress measurements in low density HMX, in: S.C. Schmidt, J.W. Shaner, G.A. Samara, M. Ross (Eds.), American Institute of Physics (AIP) Conference Proceedings, 1993.

[12] R.L. Gustavsen, S.A. Sheffield, Double shock initiation of the HMX based explosive EDC-37, in: AIP Conference Proceedings, 2002.

[13] S.A. Sheffield, R.L. Gustavsen, R.R. Alcon, In-situ magnetic gauging technique used at LANL-method and shock information obtained, in: M.D. Furnish, L.C. Chhabildas, R.S. Hixson (Eds.), Shock Compression of Condensed Matter, 1999, American Institute of Physics, New York, 2000, pp. 1043−1050.

[14] R.R. Alcon, R.N. Mulford, Shock tracker configuration of in-material gauge, in: S.C. Schmidt, W.C. Tao (Eds.), Shock Compression of Condensed Matter 1995, American Institute of Physics, New York, 1996, pp. 1057−1060.

[15] R.R. Alcon, S.A. Sheffield, A.R. Martinez, R.L. Gustavsen, Magnetic gauge instrumentation on the LANL gas-driven two-stage gun, in: S.C. Schmidt, D.P. Dandekar, J.W. Forbes (Eds.), Shock Compression of Condensed Matter 1997, 1998.

[16] R.L. Gustavsen, S.A. Sheffield, R.R. Alcon, Low pressure shock initiation of porous HMX for two grain size distributions and two densities, in: S.C. Schmidt, W.C. Tao (Eds.), Shock Compression of Condensed Matter 1995, American Institute of Physics, New York, 1996, pp. 851−854.

[17] R.L. Gustavsen, S.A. Sheffield, R.R. Alcon, Detonation wave profiles in HMX based explosives, in: S.C. Schmidt, D.P. Dandekar, J.W. Forbes (Eds.), Shock Compression of Condensed Matter 1997, American Institute of Physics, New York, 1998, pp. 739−742.

[18] R.L. Gustavsen, S.A. Sheffield, R.R. Alcon, L.G. Hill, R.E. Winter, et al., Initiation of EDC-37 measured with embedded electromagnetic particle velocity gauges, in: M.D. Furnish, L.C. Chhabildas, R.S. Hixson (Eds.), Shock Compression of Condensed Matter, 1999, American Institute of Physics, New York, 2000, pp. 879−882.

[19] W.F. Hemsing, Velocity sensing interferometer (VISAR) modification, Rev. Sci. Instrum. 50 (1) (1979) 73−78.

[20] E. Barsis, E. Williams, C. Skoog, Piezoresistivity coefficients in manganin, J. Appl. Phys 41 (1980) 5155−5162.

[21] S.C. Gupta, Y.M. Gupta, Piezoresistive response of longitudinally and laterally orientated ytterbium foils subjected to impact and quasi-static loading, J. Appl. Phys. 57 (1986) 2464−2473.

[22] Z. Rosenberg, Y. Partom, Lateral stress measurement in shock-loaded targets with transverse piezoresistive gauges, J. Appl. Phys. 58 (1985) 3072−3076.

[23] J.C. Millett, N.K. Bourne, Z. Rosenberg, On the analysis of transverse stresses during shock loading experiments, J. Phys. D: Appl. Phys. 29 (1996) 2466−2472.

[24] J.A. Charest, C.S. Lynch, The response of PVF2 stress gauges to shock wave loading, in: S.C. Schmidt, J.N. Johnson, L.W. Davidson (Eds.), Shock Compression of Condensed Matter 1989, Elsevier, Amsterdam, 1990, pp. 797−800.

[25] J.A. Charest, C.S. Lynch, A simple approach to piezofilm stress gauges, in: S.C. Schmidt, et al. (Eds.), Shock Compression of Condensed Matter 1991, North-Holland, Amsterdam, 1992, pp. 897−900.

[26] D.B. Hayes, Polymorphic phase transformation in shock-loaded potassium chloride, J. Appl. Phys. 45 (1974) 1208−1217.

[27] Z. Rosenberg, D. Yaziv, Y. Partom, Direct measurement of strain in plane impact experiments by a longitudinal resistance gauge, J. Appl. Phys. 51 (1980) 4790−4798.

[28] R.N. Mulford, R.R. Alcon, Shock initiation of PBX-9502 at elevated temperatures, in: S.C. Schmidt, W.C. Tao (Eds.), Shock Compression of Condensed Matter 1995, American Institute of Physics, New York, 1996, pp. 855−858.

[29] S.A. Sheffield, R.L. Gustavsen, R.R. Alcon, Observations of shock-induced reaction in liquid bromoform up to 11 GPa, in: S.C. Schmidt, W.C. Tao (Eds.), Shock Compression of Condensed Matter 1995, American Institute of Physics, New York, 1996, pp. 771−774.

[30] S.A. Sheffield, R.L. Gustavsen, R.R. Alcon, Hugoniot and initiation measurements on TNAZ explosive, in: S.C. Schmidt, W.C. Tao (Eds.), Shock Compression of Condensed Matter 1995, American Institute of Physics, New York, 1996, pp. 879−882.

[31] S.A. Sheffield, R.L. Gustavsen, R.R. Alcon, Porous HMX initiation studies—sugar as an inert simulant, in: S.C. Schmidt, D.P. Dandekar, J.W. Forbes (Eds.), Shock Compression of Condensed Matter 1997, American Institute of Physics, New York, 1998, pp. 575−578.

[32] L.L. Davis, S.A. Sheffield, R. Engelke, Detonation properties of bromonitromethane, in: M.D. Furnish, L.C. Chhabildas, R.S. Hixson (Eds.), Shock Compression of Condensed Matter 1999, American Institute of Physics, New York, 2000, pp. 785−788.

[33] J.J. Dick, Stress−strain response of PBX 9501 below 1 gigapascal from embedded magnetic gauge data using Lagrangian analysis, in: M.D. Furnish, L.C. Chhabildas, R.S. Hixson (Eds.), Shock Compression of Condensed Matter, American Institute of Physics, New York, 2000, pp. 683−686.

[34] L.J. Wen, Z.P. Duan, Z.Y. Zhang, F.L. Huang, Experimental study build-up difference of HMX and TATB based PBX explosive, Explos. Shock Wave 26−32 (2013).

[35] Z.P. Li, X.P. Long, Y.M. Huang, B. He, et al., Experimental method and application of electromagnetic particle velocity technique, Energy Mater. 13 (6) (2005) 359−361.

[36] Z.P. Li, X.P. Long, Y.M. Huang, B. He, et al., Initiation of JOB-9003 explosive study with electromagnetic particle velocity technique, Explos. Shock Wave 26 (3) (2006) 269−272.

[37] S.P. Wang, Study of electromagnetic particle velocity technique, Det. Shock Wave 4 (1) (1985) 33−35.

[38] C. Yu, Shock Hugoniot relation of JB-9001 high explosive, Chin. J. High Press. Phys. 12 (1) (1998) 72−77.

[40] M.B. Boslough, T.J. Ahrens, Particle velocity experiments in anorthosite and gabbro, Amsterdam: North-Holland, in: J.R. Asay, R.A. Graham, G.K. Straub (Eds.), Shock Compression of Condensed Matter, 1990, pp. 525−530.

[41] S.T. Stewart, T.J. Ahrens, Shock wave propagation in porous ice, in: M.D. Furnish, L.C. Chhabildas, R.S. Hixson (Eds.), Shock Compression of Condensed Matter, American Institute of Physics, New York, 2000, pp. 1241−1244.

[42] L.M. Barker, R.E. Hollenbach, Shock-wave studies of PMMA, fused silica and sapphire, J. Appl. Phys. 41 (10) (1970) 4208−4226.